A New Approach to the Analysis of the Thermal Equilibration of Optically Excited States

Mechanisms and rates of relaxation of optically excited states are important in the study of almost every material. They often determine the efficiency of some desired photoeffect and usually carry interesting information about the excited states themselves. Many fluorescent systems have been analyzed on the basis of the "universal relationship" introduced by Kennard and by Stepanov (K-S). These analyses frequently claim experimental confirmation of the applicability of the fundamental K-S assumption, namely, that the manifold of states associated with an excited electronic state have reached thermal equilibrium by the time of emission. The K-S prediction is that a certain function $F(\nu)$ will be linear in ν with slope $-h/k_BT$, where T is the ambient temperature. A more precise look at the K-S function, reported here, reveals the possibility of extensive lack of excited-state thermal equilibration. The spectral K-S temperature $T^*(\nu) = -(h/k_B)/(dF/d\nu)$ is introduced, and it is found to be seldom close to T in a sampling of spectral data from various systems. While $T^*(\nu)$ does not necessarily represent an actual molecular temperature, its variation can be modeled in broadband systems by assuming coupled emitting and absorbing submanifolds that are demonstrably far from the equilibrium envisaged by Kennard and Stepanov.

Introduction

Kennard[1] was probably the first to predict the following general relation between the shapes of the absorption and fluorescence spectra of a homogeneous substance:

$$F(\nu) = \ln\left(\frac{c^2}{8\pi h}\frac{I(\nu)}{\nu^3\sigma(\nu)}\right) = -\frac{h\nu}{k_BT} + D(T). \qquad (1)$$

Here $I(\nu)$ is the emissive power ($W\cdot Hz^{-1}$) at frequency ν, $\sigma(\nu)$ the absorption cross section at that frequency, T the ambient temperature, and $D(T)$ a quantity independent of frequency. Stepanov[2] revived interest in the relation in 1957, and it has been widely attributed to him. Others have developed the concept and formulated it for organic molecules, photosynthetic systems, semiconductors, and inhomogeneous systems.[3–7] Its application has generally focused on the goodness of the fit of experimental data to the linear function of frequency suggested by Eq. (1), and the translation of the results into a judgment of how well the excited state has attained thermal equilibrium before emission.

In Stepanov's version of the theory, relation (1) will hold if two conditions are satisfied: first, the aforementioned equilibrium, and second, that "non-exciting absorption" (due to transitions between two vibrational levels of the ground state) is negligible. The relation is frequently violated, and we shall see that these two assumptions alone do not give one a sufficiently broad basis to understand the violations.

Original Theory

Equation (1) is very general, but since it is known and applied largely by workers in biofluorescence, we review its derivation. It is a result of applying the Einstein A-B relation to sets of transitions (Fig. 67.21) in a system characterized by a metastable excited-state population. In the intensity, temperature, and wavelength regimes of interest, stimulated emission is entirely negligible. Thus[2,3]

$$\frac{I(\nu)}{\sigma(\nu)} = \frac{Z\int g'(w')A(w',\nu)p(w')dw'}{Z'\int g(w)B(w,\nu)\exp(w/k_BT)dw}, \qquad (2)$$

where g and g' are the ground- and excited-state densities of states, respectively; Z and Z' are the partition functions for the ground and excited manifolds, respectively; and A and B are the Einstein coefficients. The important function $p(w')$ is proportional to the probability of occupation of the states at w' and will be central to our subsequent discussion. When the A-B relation is introduced with concern for densities of states,

$$g'(w')A(w',\nu)dw' = \frac{8\pi h\nu^3}{c^2}g(w)B(w,\nu)dw, \qquad (3)$$

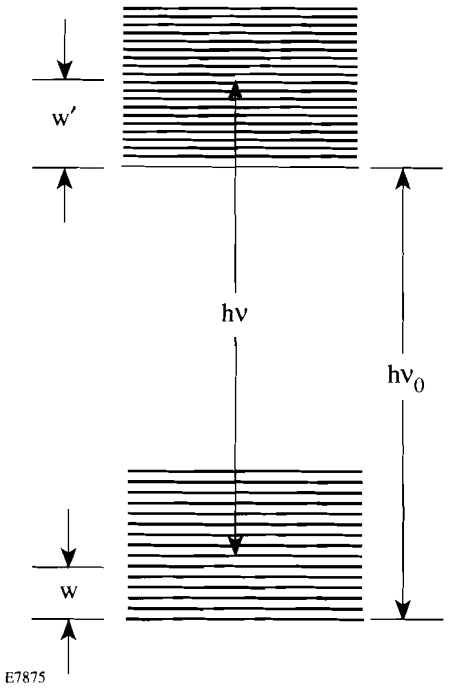

Figure 67.21
Relative positions of the energy levels involved in constructing Eq. (5), showing a transition at energy $h\nu$ between two different vibrational sublevels of the ground (w) and excited (w') states.

we obtain

$$\frac{c^2}{8\pi h}\frac{I(\nu)}{\nu^3\sigma(\nu)} = \frac{Z\int g(w)\,B(w,\nu)\,p(w')dw}{Z'\int g(w)\,B(w,\nu)\exp(-w/k_BT)\,dw}. \quad (4)$$

At each ν, the states in the vicinity of w' are connected to specific groups of states in the vicinity of w in the lower manifold, and their energies are related by

$$h\nu_0 + w' = h\nu + w; \quad (5)$$

therefore,

$$\frac{c^2}{8\pi h}\frac{I(\nu)}{\nu^3\sigma(\nu)} = \frac{Z\int g(w)\,B(w,\nu)\,p(w+h\nu-h\nu_0)\,dw}{Z'\int g(w)\,B(w,\nu)\exp(-w/k_BT)\,dw}. \quad (6)$$

Equation (6) is still quite general, and, when p is replaced by the Boltzmann distribution and $h\nu_0$ is set equal to zero, it reduces to the Wien law at photon frequencies of interest to us. What distinguishes the fluorescent case from the blackbody case is that the fluorescence has an artificially induced metastable population based on the energy $h\nu_0$ (such as, for example, the 0-0 electronic energy separation in a complex molecule). Kennard and Stepanov assumed such a metastable situation in a fluorescent system and made the further key assumption that the excited system was thermally equilibrated:

$$p(w') = \exp(-w'/k_BT) = \exp\left[-(w+h\nu-h\nu_0)/k_BT\right]. \quad (7)$$

Introduction of this distribution into Eq. (6) leads immediately to Eq. (1) and tells us that the quantity $D(T)$ is the system-specific quantity $h\nu_0/k_BT + \ln(Z/Z')$. The careful identification of $D(T)$ is due to Neporent.[3]

Ordinarily, the relation (1) is checked for a substance by finding the slope of $F(\nu)$ from experimental data and comparing T, as determined from this slope, with the ambient temperature. The most reliable data are those from the Stokes region, where both absorption and emission are at a high fraction of their maximum values. Experimenters have almost always found the relationship to be "half-right"—the function $F(\nu)$ is a reasonably straight line over much of the Stokes region, but, remarkably, the deduced value of T has seldom agreed with the ambient temperature. In Fig. 67.22, taken from

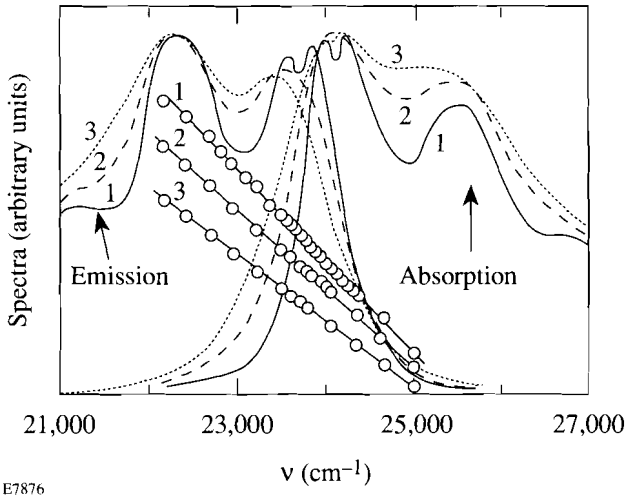

Figure 67.22
Absorption and emission spectra of perylene vapor at (1) 513 K, (2) 633 K, and (3) 713 K, and the corresponding Kennard-Stepanov functions (straight lines). Note the correct qualitative temperature dependence of the slope of $F(\nu)$. These straight lines cover over three decades on the vertical scale and yield effective temperatures 556 K, 655 K, and 755 K, respectively. After Borisevich and Gruzinskii.[8]

Borisevich and Gruzynskii,[8] it is seen that the effective temperature T^* deduced from the slope is 20 K to 60 K higher than ambient. In some cases T^* has been as high as twice ambient temperature; in a few cases it has been lower. There has been much speculation as to the causes of these particular deviations from the relation. Many cases are reviewed and discussed by Van Metter and Knox,[6] who evaluated inhomogeneous broadening as a possible cause.

Alternative Approach

The observed linear function that remarkably arises from very complex input is a broad confirmation of the "universal relation," but its failure in detail is symptomatic of the possibility of a very complex nonequilibrium distribution during the lifetime of the fluorescence. The experiments yielding $T^* \neq T$ seem to tell us that this distribution is nearly equilibrated, although the conclusion that the excited molecule has a "warm" environment is inconsistent with a single temperature appearing in the theory.[6] Here we report a new method of analyzing the Kennard-Stepanov data that highlights the deviation from a Boltzmann distribution. We find that the failure of the slope to produce an ambient temperature value is only one aspect of this deviation, and we set forth a phenomenological theory on the basis of which some of the observations can be understood.

We define the Kennard-Stepanov spectral temperature in terms of the local slope of $F(\nu)$:

$$T^*(\nu) \equiv -\left[\frac{k_B}{h}\frac{dF(\nu)}{d\nu}\right]^{-1}$$

$$= -\left\{\frac{k_B}{h}\frac{d}{d\nu}\ln\left[\frac{c^2}{8\pi h}\frac{I(\nu)}{\nu^3\sigma(\nu)}\right]\right\}^{-1}. \qquad (8)$$

This device transforms the rather prosaic experimental $F(\nu)$ into a spectrum which, in most cases seen to date, is rich in detail. There are peaks, valleys, plateaus, and sometimes divergences. In virtually no case to date have we found a constant $T^*(\nu)$, as the K-S relation predicts. $T^*(\nu)$ curves computed from data sets in several typical cases[9–12] are shown in Fig. 67.23. A frequently seen feature is that $T^*(\nu)$ remains fairly constant either near ambient temperature or somewhat above it over much of the frequency range but includes one or more peaks.

In practice, $T^*(\nu)$ is found from the inverse slope of the regression line through $F(\nu)$ for a series of data points centered at frequency ν. The width of the derivative window can be

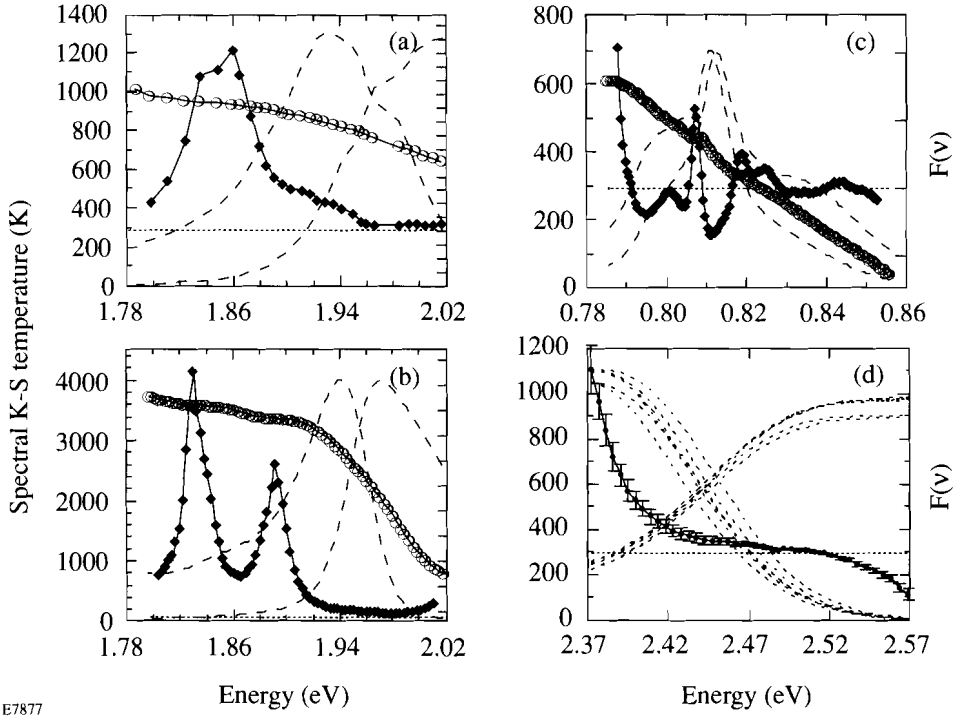

Figure 67.23
Experimental $T^*(\nu)$ spectra (filled diamonds) and the parent $F(\nu)$ (open circles). Dashed curves in the background are emission (on the left) and absorption (on the right). Spectra are in arbitrary units, $T^*(\nu)$ is in K, and the variation of $F(\nu)$ is indicated by tick marks, separated by factors of 2.303, at the right of each frame except (d). The abscissa is frequency in energy units. (a) α-phycocyanin, 295 K (K. Sauer[9]); (b) α-phycocyanin, 77 K (M. Debreczeny *et al.*[10]); (c) erbium-doped silicate glass, 295 K (R. Giles and DeSurvire[11]); (d) poly(*p*-phenylene vinylene), PPV.[12] In each case the constant value of the ambient temperature, which is the prediction of the universal relation for T^*, is shown as a horizontal dotted line. In (d), the spectral temperature computed from six absorption-emission pairs is shown as a mean with standard deviation indicated by error bars.

varied. A larger window is necessary when there seems to be a great deal of experimental noise. In most cases, the slope has been best found over a number of data points ranging between 5 and 11. Generally, changing the width of the derivative window has only a very slight effect upon the contour of $T^*(\nu)$. By introducing artificial noise and artificial miscalibrations into simulated data, we have satisfied ourselves that the structures seen are not artifacts of the method. Also, the effects appear to be reproducible, as will be discussed.

Before discussing the possible origins of the structure appearing in Fig. 67.23, we describe the materials on which it is based. We have found it difficult to rely on the published literature for the accuracy necessary in this study, so in most cases unpublished data in electronic form have been used. Figures 67.23(a) and 67.23(b) refer to solutions of a subunit of an important photosynthetic antenna protein, α-phycocyanin (α-PC). Figure 67.23(a) shows one of the first cases we analyzed. Kenneth Sauer,[9] who brought its unusual K-S behavior to our attention several years ago, computed $F(\nu)$ from room-temperature fluorescence and absorption spectra of α-PC representative of samples from four different organisms (Switalski[13]). The four α-PC had similar fluorescence, absorption, and circular dichroism spectra, similar time-resolved fluorescence behavior, and high fluorescence polarization across the entire band of excitation wavelengths. Care was taken to test for the presence of α-β heterodimers.

The data from which Fig. 67.23(b) was produced were those of Debreczeny and colleagues.[10] Again the system is the subunit α-PC, this time at 77 K in a buffer of 5 mM phosphate at pH 7.0 with 75% glycerol by volume. The small rise near 2.02 eV should be ignored as it may be a result of scattering from the 560-nm excitation source.

Figures 67.23(c) and 67.23(d) show K-S analyses for two materials of interest to applied physics. The former represents room-temperature Er-doped silicate glass co-doped with Al and Ge,[11] one of the important materials for use in fiber light amplifiers. The latter shows spectral temperatures computed from the spectra of a series of poly(p-phenylene vinylene) (PPV) samples,[12] materials of interest for use in light-emitting diodes. The several cases shown represent data from samples subjected to different periods of aging. The case of Fig. 67.23(c) illustrates the remarkable amount of structure that sometimes presents itself in terms of a K-S spectral temperature. Figure 67.23(d) will be discussed later as an example of reproducibility of the curves.

Model Calculations

The existence of peaks in certain $T^*(\nu)$ data may be understood physically on the basis of the following straightforward model. A system of fluorescing states is considered as a mixture of individual systems within each of which there is thermal equilibration and among which detailed-balance kinetics with adjustable rates can be applied. This is a natural development of an idea introduced by Band and Heller.[7] In terms more closely related to our context, each subsystem of fluorescers is a "K-S system" that contributes absorption and fluorescence components obeying Eq. (1) but whose populations relative to each other are kinetics-dependent. The subsystems may in fact be chemically different molecules or sets of chemically identical molecules that are inhomogeneously broadened, or they may represent manifolds associated with different electronic states of each molecule of a homogeneous species.

It is readily shown that the K-S function for the K-S mixture just described is given by

$$F(\nu) = \ln\left\{\sum_i \bar{p}_i \xi_i(\nu) \exp\left[F_i(\nu)\right]\right\}, \tag{9a}$$

where $\bar{p}_i$ is the average relative population of the emitting subset i, $F_i(\nu)$ is the K-S function for that subset, and

$$\xi_i(\nu) = \frac{\sigma_i(\nu)}{\sum_j \sigma_j(\nu)}. \tag{9b}$$

From this, we can discern that, for a system in which the absorption and emission spectra are linear combinations of the individual spectra of n species, each of which obey Eq. (1), $F(\nu)$ will have n asymptotes of slope $-h/k_BT$. In a mixture of two species that do not exchange excitation energy (noninteracting species), the spacing between the intercepts will be equal to the difference between the two values of $D(T)$. The two asymptotes of $F(\nu)$ can be seen clearly in Fig. 67.24(a), which depicts the partially resolved absorption and fluorescence spectra along with $F(\nu)$ and $T^*(\nu)$ associated with two manifolds that are not exchanging excitation energy. These manifolds are represented by Gaussian absorption peaks centered at 1.810 and 1.851 eV, each with 17-meV FWHM. Since the manifolds correspond to "good K-S systems," the two emission bands are automatically determined.

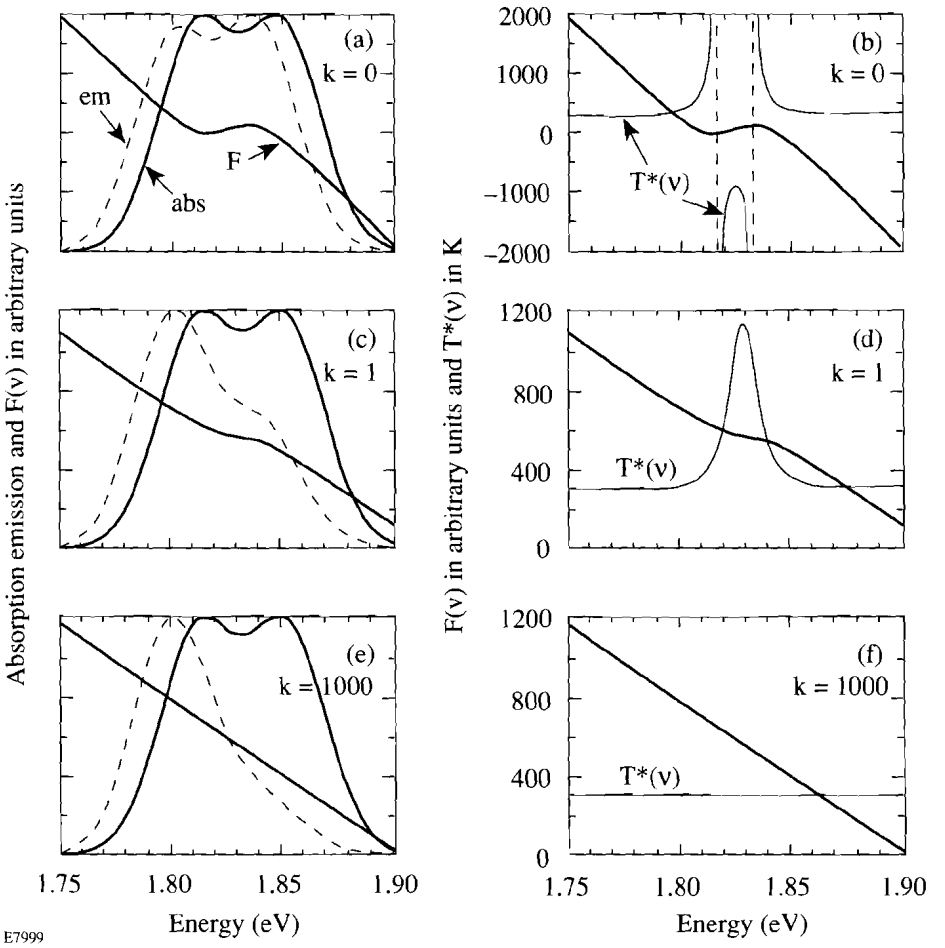

Figure 67.24
Results of a model calculation of $F(v)$ and $T^*(v)$ for two manifolds interchanging populations with rate constants k, downward, and $k\exp(-\Delta/k_BT)$, upward. $F(v)$ curves, heavy line, are shown in all parts of the figure; the spectra from which they derive are shown in (a), (c), and (e), and $T^*(v)$ is shown as indicated in (b), (d), and (f). The total dipole strength is the same in each spectral manifold and is distributed as two resolved Gaussian absorption and emission bands. The absorption FWHM of the individual bands, whose centers are located at 1.810 and 1.851 eV, is 17 meV. The total absorption and emission are shown as thin solid and dashed lines, respectively, adjusted to full scale. The lifetime of each manifold is taken to be 1.0 ns and k is expressed in units of $(1.0\ \text{ns})^{-1}$. Broadband excitation is assumed. As k increases, top to bottom, the kink in the $F(v)$ curve flattens out and $T^*(v)$ progresses from divergent (b), to peaked (d), to constant (f).

Exchange of excitation between the manifolds makes the situation slightly more complex. We solve the kinetic equations for the steady-state manifold populations $\bar{p}_i$, assuming that the exciting light is constant and using transfer rates, intrinsic quantum yields, relative oscillator strengths, and spectral shape functions as inputs. We assume a rate k for transfer from the upper to the lower manifold and, in keeping with detailed balance, a rate $k\exp(-\Delta E/k_BT)$ from lower to upper. For our particular spectra, $\exp(-\Delta E/k_BT) = 0.145$ at $T = 300$ K. In each manifold we take $Z = Z'$ and unit quantum yield for simplicity. Figures 67.24(c) and 67.24(e) illustrate the effect of increasing k; the curvature in $F(v)$ is completely smoothed out as k reaches 1000 times the fluorescence rate. Correspondingly, as one may see by scanning Figs. 67.24(b), 67.24(d), and 67.24(f) from top to bottom, there is a dramatic effect on $T^*(v)$ as the excited state approaches an equilibrium condition. At the same time, one sees the emission shifting from an equal mixture of both bands [Fig. 67.24(a)] to predominant emission from the lower band [Figs. 67.24(c) and 67.24(e)]. A peak in $T^*(v)$ appears at relatively small excitation exchange rate, which is a significant result. To the extent that such modeling is appropriate, it appears to indicate that the various systems involved in Fig. 67.24 exhibit considerable nonequilibration preceding fluorescence. A more extensive range of parameters has been studied[14] and further work is planned.

More generally, there will be at most $n-1$ peaks in $T^*(v)$ for n excited manifolds. These peaks correspond to the visibly nonlinear portions between the asymptotes of $F(v)$. When $F(v)$ includes one or more segments of positive slope, $T^*(v)$ will be undefined where the slope momentarily crosses zero, and may become negative, as in Fig. 67.24(b). The number of species present is not necessarily evident from looking at a plot of $T^*(v)$ because some of the peaks may be small enough to be indistinguishable from experimental noise or two or more peaks may be so close together that they resemble one.

Discussion

The full modeling of spectra must account also for $T^*(\nu)$ dropping below ambient, in some cases becoming divergent. Our exploration of parameter space has shown that dips below ambient are indicative of the higher-energy species having a low quantum yield, and that divergences occur when there is broadband excitation of weakly coupled manifolds whose separation is greater than their widths. Variation in the curves with excitation wavelength is readily treated with the kinetic model, in analogy with the variation of the standard T^*, discussed and reviewed by Van Metter and Knox.[6] Variation of the standard T^* was observed in splendid detail recently by Sechkarev and Beger[15] in adsorbed rhodamine 6G, a system for which the present method should provide an even richer basis for analysis of the relaxation.

The systems of Fig. 67.23 are complex, and we have had only limited success in fitting the curves using this elementary relaxation model. The α-PC peaks in Figs. 67.23(a) and 67.23(b) are sufficiently stable and reproducible that the existence of poorly coupled states, as in our model, is a good possibility. Should they represent impurities, it is clear that the K-S analysis is a sensitive method for locating them. The T^* variations of Figs. 67.23(c) and 67.23(d) may well be indicative of single-manifold K-S failure. Another consideration is inhomogeneous broadening,[6] which, in a case involving a single species, causes an upward shift in the value of the ordinary T^* and, if the excitation is not broadband, introduces some weak ν dependence into $T^*(\nu)$. Adding inhomogeneous broadening into the computer simulation might make it possible to model a case resembling the 77 K data of Debreczeny *et al.*[10] [Fig. 67.23(b)], in which the contour of the $T^*(\nu)$ plot resembles the theoretical case of a mixture of species, but in which $T^*(\nu)$ never goes as low as the ambient temperature.

It is necessary to address the question of reproducibility of the experimental effects. Of course, this is primarily a matter of reproducibility of the spectra involved, but $T^*(\nu)$ senses small relative changes, in analogy with derivative spectroscopy. In the case of α-phycocyanin, Debreczeny's 295 K data (not shown) is very similar to Sauer's [Fig. 67.23(a)], a main peak occurring at 1.87 eV and an additional one outside Sauer's range at 1.80 eV. As the temperature is lowered, these peaks apparently shift and interchange strengths, ending up at 1.89 and 1.83 eV at 77 K [Fig. 67.23(b)]. The data on PPV [Fig. 67.23(d)] provide a good example of $T^*(\nu)$ reproducibility. The several dashed curves shown are absorption and emission spectra of six different samples. While in this case the data come from the same laboratory,[12] each sample was grown from a different precursor aged for six separate periods of time. When judging reproducibility, we must recognize that the utility of the $T^*(\nu)$ analysis brings with it the cost of high sensitivity to those experimental conditions that affect equilibrium among various manifolds of states.

Conclusions

We have shown the usefulness of plotting a new function $T^*(\nu)$ in order to magnify regions of nonlinearity in the K-S function that analyzes equilibration in fluorescing excited states. The nonlinearity of these plots has long been smoothed over in their interpretation. As we have seen, however, peaks in $T^*(\nu)$ could be sensitive indicators of the presence of hidden excited states or impurities with which there is incomplete thermal equilibration. $T^*(\nu)$ should prove useful as a means of estimating transfer rates in complex molecules. We are persuaded by the data and by several preliminary theoretical results that our interpretation is correct, and that efforts to examine the full parameter space will be rewarded.

ACKNOWLEDGMENT

We thank Kenneth Sauer and Martin Debreczeny for helpful correspondence and for supplying the unpublished data of Figs. 67.23(a) and 67.23(b). C. Randy Giles kindly supplied the published data of Fig. 67.23(c) in electronic format. Matt Robinson and Yongli Gao kindly provided a prepublication copy of Ref. 12 and the data of Fig. 67.23(d). We acknowledge the lively discussions with Philip Laible and Thomas Owens that helped launch this project. The research was sponsored in part by the U. S. Department of Agriculture, NRI Competitive Grants Office project 95-37306-2014, and in part by the National Science Foundation under grants 94-00059 and 94-15583.

REFERENCES

1. E. H. Kennard, Phys. Rev. **11**, 29 (1918); Phys. Rev. **28**, 672 (1926).
2. B. I. Stepanov, Sov. Phys. Dokl. **2**, 81 (1957).
3. B. S. Neporent, Sov. Phys. Dokl. **3**, 337 (1958).
4. R. T. Ross, Photochem. Photobiol. **21**, 401 (1975).
5. D. E. McCumber, Phys. Rev. **136**, A954 (1964).
6. R. L. Van Metter and R. S. Knox, Chem. Phys. **12**, 333 (1976).
7. Y. B. Band and D. F. Heller, Phys. Rev. A **38**, 1885 (1988).
8. N. A. Borisevich and V. V. Gruzinskii, Opt. Spectrosc. **14**, 20 (1963).

9. K. Sauer, unpublished data (1987).

10. M. P. Debreczeny *et al.*, J. Phys. Chem. **97**, 9852 (1993); J. Phys. Chem. **99**, 8412 (1995).

11. C. R. Giles and E. Desurvire, J. Lightwave Technol. **9**, 271 (1991).

12. M. R. Robinson *et al.*, Polym. Mater. Sci. Eng. **74**, 292 (1996).

13. S. C. Switalski and K. Sauer, Photochem. Photobiol. **40**, 423 (1984); S. C. Switalski, Ph. D. thesis, University of California, Berkeley, 1986.

14. D. A. Sawicki and R. S. Knox, Phys. Rev. A (in press).

15. A. V. Sechkarev and V. N. Beger, Opt. Spectrosc. **72**, 303 (1992).